Decay Modes of Giant Resonances in ^{58}Ni, ^{60}Ni, and ^{62}Ni

E. Wolynec,[a] W. R. Dodge, and E. Hayward
National Bureau of Standards, Washington, D. C. 20234
(Received 1 November 1978)

The (e,p) and (e,α) cross sections for targets of ^{58}Ni, ^{60}Ni, and ^{62}Ni have been measured in the electron energy range 16–50 MeV. They have been analyzed using the distorted-wave Born-approximation $E1$ and $E2$ virtual-photon spectra. Protons are emitted primarily following $E1$ absorption but α emission results from a combination of $E1$ and $E2$ absorption. The $E2$ isoscalar giant resonance decays predominantly by α emission for these nuclei.

The purpose of this Letter is to point out and to illustrate with experimental data a new important advance in an old technique, namely, the use of virtual-photon spectra to determine the multipolarity of nuclear excitations. This has been made possible by the availability of the distorted-wave Born-approximation (DWBA) calculations[1,2] of the virtual-photon spectrum. These experiments have led to the interesting and somewhat surprising conclusion that, at least for the nickel isotopes, α-particle emission is the dominant decay mode of the $E2$ isoscalar giant resonance.

The electrodisintegration of ^{58}Ni, ^{60}Ni, and ^{62}Ni has been studied by measuring the energy spectra, $d^2\sigma/dT\,\Omega$, for the protons and α particles emitted at 48°, 90°, and 132° with electron bombarding energies, E_0, in the range 16–50 MeV. The decay-particle spectra peak at 5 and 8 MeV for protons and α particles, respectively, and have the asymmetric shape characteristic of Coulomb-barrier penetration. These data allowed us to determine the total cross sections, $\sigma_{e,p}(E_0)$ and $\sigma_{e,\alpha}(E_0)$. The yields, $Y_{e,p}(E_0)$ and $Y_{e,\alpha}(E_0)$, produced by both electrodisintegration and photodisintegration, when a 0.217-g/cm^2 tantalum foil was placed in the electron beam 7.6 cm ahead of the target, were also measured at a few electron energies.

The excitation functions, $\sigma_{e,x}(E_0)$, have been analyzed by making use of the $E1$ and $E2$ virtual-photon spectra. These are shown in Fig. 1 for 50-MeV electrons intereacting with a Ni nucleus. It may be seen that the $E2$ virtual-photon spectrum is much richer in giant-resonance photons than the $E1$ spectrum; and furthermore it rises much more steeply as lower virtual-photon energies are approached. These differences in the $E1$ and $E2$ virtual-photon spectra can be used to determine giant-resonance energies and strengths from the measured yield curves. Since data were taken only in two- or three-MeV steps, no information can be obtained regarding the detailed cross-section shapes.

The relationship between the electrodisintegration cross section leading to the emission of particle x, $\sigma_{e,x}(E_0)$, and the corresponding photodisintegration cross section, $\sigma_{\gamma,x}{}^{\lambda L}(E)$, is

$$\sigma_{e,x}(E_0)=\int_0^{E_0-m}\sum_{\lambda L}\sigma_{\gamma,x}{}^{\lambda L}(E)N^{\lambda L}(E_0,E,Z)E^{-1}\,dE, \tag{1}$$

where $N^{\lambda L}(E_0,E,Z)$ is the virtual-photon intensity spectrum of multipolarity λL. The measured excitation functions have been fitted by using, in Eq. (1), $E1$ and $E2$ DWBA virtual-photon spectra and various hypothetical as well as published cross sections. The latter were fitted by using an arbitrary normalization but maintaining the cross-section shapes. For the hypothetical cross sections we used a Lorentzian line modified in such a way that it has a width Γ_1 for energies below the peak energy and Γ_2 above. It turns out from the fits that $\Gamma_1<\Gamma_2$. This alteration in the conventional resonance shape may be viewed as a way of mocking the effect of the Coulomb barrier. In every case the parameters that best fit this excitation function also fit the yield, $Y_{e,x}(E_0)$, measured when the radiator was in and calculated according to

$$Y_{e,x}(E_0)=\sigma_{e,x}(E_0)+N_r\int_0^{E_0-m}\sigma_{\gamma,x}(E)K(E_0,E,Z)E^{-1}\,dE, \tag{2}$$

where N_r is the number of radiator nuclei per square centimeter and $K(E_0,E,Z)$ is the Schiff bremsstrahlung cross section.

As an example, we show in Fig. 2 the cross section for the production of protons, $\sigma_{e,p}(E_0)$, when electrons of total energy E_0 are incident on a ^{58}Ni target (open circles). The closed circles represent

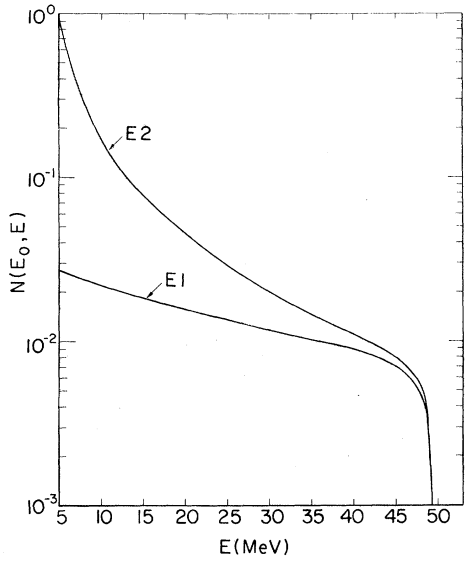

FIG. 1. The intensity spectra of $E1$ and $E2$ virtual photons generated when 50-MeV electrons are inelastically scattered by a Ni nucleus.

the yield when the radiator was placed in the incident electron beam. Curve A was obtained by folding 1.26 times the (γ,p) cross section of Ishkhanov *et al.*[3] with the $E1$ virtual-photon spectrum according to Eq. (1). Curve B was obtained by taking into account the radiator thickness according to Eq. (2). For ^{60}Ni a similar fit was obtained using 0.94 times the (γ,p) cross section of Ref. 3. The ^{62}Ni data were also fitted using the $E1$ virtual-photon spectra. Even though the protons in the low-intensity, high-energy tail of the energy spec-

TABLE I. Resonance parameters for $\sigma_{\gamma,p}$.

Nucleus	E_x (MeV)	Γ (MeV)[a]	$\int_0^{30}\sigma\,dE$ (MeV mb)	SR[b] (%)
^{58}Ni	19.2±0.5	6.5±1.3	738±40	85±5
^{60}Ni	18.5±0.5	9.2±1.8	304±20	34±2
^{62}Ni	21.0±0.5	5.8±1.0	140±10	15±1

[a] Γ is the full width at half maximum.
[b] SR stands for sum rule; the $E1$ SR equals 60 NZ/A MeV mb.

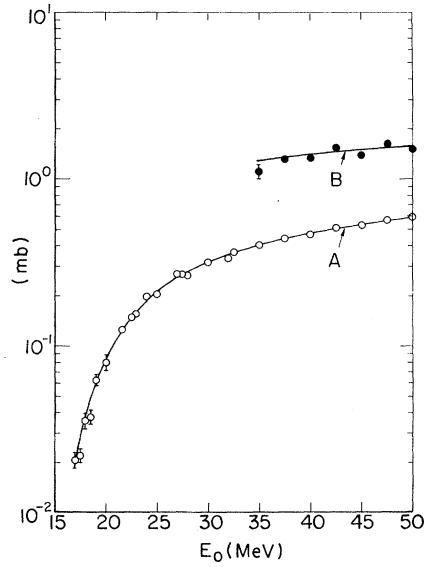

FIG. 2. The cross section for the production of protons, $\sigma_{e,p}(E_0)$, when electrons of total energy E_0 are incident on a ^{58}Ni target (open circles). The closed circles represent the yield of protons obtained when a 0.217-g/cm^2 Ta foil was placed in the incident electron beam. Curve A is predicted using 1.26 times the (γ,p) cross section of Ref. 6 along with the $E1$ virtual-photon spectra in Eq. (1). Curve B is obtained by taking into account the radiator thickness according to Eq. (2).

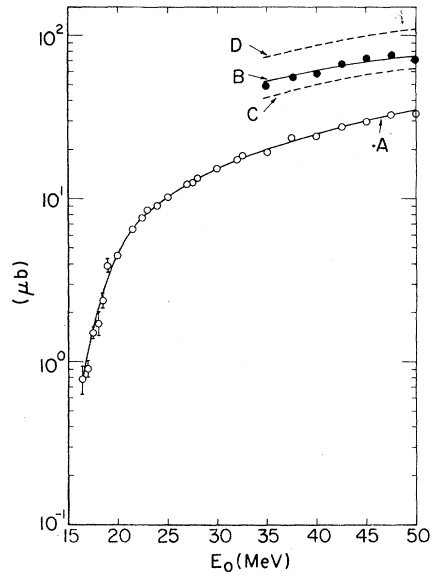

FIG. 3. The measured $\sigma_{e,\alpha}(E_0)$ (open circles) for ^{58}Ni as a function of total incident electron energy, E_0. The closed circles represent the electrodisintegration plus photodisintegration yield obtained when the 0.217-g/cm^2 tantalum foil was interposed in the incident electron beam. Curve A is the best fit to the data obtained by using the $E1$ and $E2$ virtual-photon spectra in Eq. (1) along with the two resonance lines whose parameters are given in Tables II and III. Curve B is the corresponding result with the radiator in, obtained using Eq. (2). Curve D was predicted using the best $E1$ fit to the data, a 22-MeV–wide resonance. Curve C was predicted using the best $E2$ fit to the data. This figure is intended to show that both $E1$ and $E2$ components are necessary to explain the (e,α) cross section.

TABLE II. $E1$ components in the (γ,α) reaction.

Nucleus	E_x (MeV)	Γ (MeV)[a]	$\int\sigma dE$ (MeV mb)	SR[b] (%)
^{58}Ni	18.3±0.5	6±1	15.3±1.3	1.8±0.2
^{60}Ni	21.5±1.0	6±1	18.5±1.4	2.1±0.2
^{62}Ni	18.3±1.0	5±1	4.8±0.6	0.5±0.1

[a] Γ is the full width at half maximum.
[b] $E1$ SR equals $60NZ/A$ MeV mb.

TABLE III. $E2$ components in the (γ,α) reaction.

Nucleus	E_x (MeV)	Γ (MeV)[a]	$\int\sigma dE$ (MeV mb)	SR[b] (%)
^{58}Ni	16.5±0.5	4.2±1.0	10.4±0.7	56±4
^{60}Ni	16.0±0.5	3.7±0.8	6.9±0.4	52±3
^{62}Ni	16.8±0.5	4.5±1.0	5.1±0.4	28±2

[a] Γ in the full width at half maximum.
[b] $E2$ SR equals $0.22\ Z^2/A^{1/3}$ μb/MeV.

tra from ^{60}Ni and ^{62}Ni were peaked slightly forward of 90°, the analysis using the virtual-photon spectra indicated that the (e,p) reaction in the nickel isotopes is predominantly an electric dipole phenomenon. The resonance parameters for the hypothetical (γ,p) cross sections that best fit our data are given in Table I.

The (e,α) cross sections, on the other hand, have both $E1$ and $E2$ components. We illustrate this result in Fig. 3 where $\sigma_{e,\alpha}(E_0)$ for ^{58}Ni is plotted as a function of total incident electron energy (open circles) along with the yields obtained using the radiator (closed circles). Curve A is the best fit to the data using the $E1$ and $E2$ virtual-photon spectra in Eq. (1) along with the hypothetical resonance lines whose parameters are given in Tables II and III. When only $E1$ excitations were postulated, the cross section was 22 MeV wide, which is totally unreasonable, and the yield predicted with the radiator in (curve D) was much too large. The best fit for pure $E2$ absorption is not statistically acceptable and predicts curve C if the radiator is in. Both $E1$ and $E2$ components must, therefore, be included to explain the (e,α) cross sections. The $E1$ and $E2$ resonance energies and widths necessary to explain the (e,α) data for the three targets, ^{58}Ni, ^{60}Ni, and ^{62}Ni, are given in Tables II and III. The quoted errors represent uncertainties in the fits based only on the counting statistics and do not include errors resulting from the use of an artificial resonance line along with the DWBA virtual-photon spectra in Eq. (1). In every case the appropriate yield was obtained using Eq. (2) for the yield with the radiator in.

The $E1$ part of the (γ,α) cross section is, of course, a very small fraction of the total $E1$ absorption cross section. The $E2$ (γ,α) cross section, on the other hand, accounts for more than half of the energy-weighted isoscalar sum for ^{58}Ni and ^{60}Ni. When compared with the values of 55% and 63% obtained in the (α,α') experiments,[4] we are led to the conclusion that α emission is by far the dominant decay mode for the $E2$ isoscalar resonance. This possibility has already been suggested by Flowers *et al.*[5] in connection with a similar experiment.

We are aware that this conclusion is in conflict with the inference drawn from the ^{58}Ni$(\alpha,\alpha'\alpha'')$ and ^{58}Ni$(\alpha,\alpha'p)$ coincidence experiments,[6,7] and suggest that the resolution of this discrepancy could lie in the recognition that the α-particle projectile cannot be a pure isoscalar object,[8] nor can the target that it polarizes.[9] A complete paper giving more details and comparisons with other data is in preparation.

The authors wish to thank S. Penner and E. G. Fuller for their continued interest in this experiment and for many fruitful discussions. This work was supported in part by Foundacao de Amparo a Pesquisa do Estodo de São Paulo.

[a]On leave from the University of São Paulo, São Paulo, Brazil.

[1]W. W. Gargaro and D. S. Onley, Phys. Rev. C 4, 1032 (1971).

[2]C. W. Soto Vargas, D. S. Onley, and L. E. Wright, Nucl. Phys. A288, 45 (1977).

[3]B. S. Ishkanov, I. M. Kapitonov, I. M. Piskarev, V. G. Shevchenko, and O. P. Shevchenko, Yad. Fiz. 11, 485 (1970) [Sov. J. Nucl. Phys. 11, 272 (1970)].

[4]D. H. Youngblood, J. M. Moss, C. M. Rozsa, A. D. Bacher, and D. R. Brown, Phys. Rev. C 13, 994 (1976).

[5]A. G. Flowers, A. C. Shotter, D. Branford, J. C. McGeorge, and R. O. Owens, Phys. Rev. Lett. 40, 709 (1978).

[6]K. T. Knöpfle, H. Riedesel, K. Schindler, G. J. Wagner, C. Mayer-Böricke, W. Oelert, M. Rogge, and P. Turek, to be published.

[7]M. T. Collins, C. C. Chang, S. L. Tabor, J. R. Wu, and M. D. Glascock, Bull. Am. Phys. Soc. 23, 506 (1978).

[8]M. Gell-Mann and V. L. Telegdi, Phys. Rev. 91, 169

(1953).

[9]M. Danos, in *Proceedings of the International Conference on Photonuclear Reactions and Applications, Pacific Grove, California, 1973,* edited by B. L. Berman (Lawrence Livermore Laboratory, Livermore, Calif., 1973), Vol. I, p. 436.

Nucleon Scattering from Mo Isotopes and the Lane Model

J. R. Comfort

Department of Physics and Astronomy, University of Pittsburgh, Pittsburgh, Pennsylvania 15260

(Received 18 September 1978)

A unified optical-model analysis of neutron and proton elastic scattering from Mo isotopes reveals breakdowns of the Lane model of $\vec{t}\cdot\vec{T}$ interactions, most clearly evident as shell effects. The puzzle is that a coupled-reaction-channel reanalysis does not remove these.

Recent analyses of neutron elastic-scattering data[1,2] on Mo isotopes have revealed some inconsistencies with the Lane model of $\vec{t}\cdot\vec{T}$ interactions.[3] The $(N-Z)$ dependence of the imaginary potential was opposite to that of the real potential, in contrast to the usual expectations. Problems have also been noted in the application of the Lane model in (p,n) reactions on molybdenum.[4]

The recent availability of excellent neutron-scattering data, in conjunction with existing proton-scattering data, enables more sensitive analyses of small effects in the scattering mechanisms. The Mo isotopes are especially appropriate for these. The asymmetry $\epsilon = (N-Z)/A$ nearly doubles between ^{92}Mo and ^{100}Mo. Inelastic-scattering cross sections to the lowest 2^+ states also increase by about a factor of 5, yet this onset of collectivity does not entirely mask shell effects.

A study of the influence of nuclear structure on nucleon scattering, and the implications for the Lane model, is reported here. Both neutron and proton scattering from even Mo isotopes are analyzed consistently with common geometries for the potentials. The best optical-model (OM) results for the volume integrals are inconsistent in significant ways with the predictions of the Lane model. An important discrepancy is the evidence for pronounced shell effects in the scattering from ^{92,100}Mo, very prominent for protons but nearly absent for neutrons. Couplings with deuteron intermediate channels are suggested. Coupled-reaction-channel (CRC) calculations are made that include couplings to 2^+ and 3^- states via inelastic scattering and to deuteron intermediate channels via pickup reactions, and the elastic data are refitted. Somewhat better consistency with the Lane model is found, but the shell effects remain large.

Elastic-scattering cross sections for 11-MeV neutrons from ^{92,96,98,100}Mo were obtained from Rapaport *et al.* and are described elsewhere.[1] They are corrected for very small compound-nucleus contributions and have absolute scales known to within 5%. Cross sections for 15-MeV protons on ^{92,94,96,98,100}Mo were measured with a ruler from enlarged figures from Lutz, Heikkinen, and Bartonlini,[5] the numbers being no longer extant. Normalizations had originally been made to the optical model. Inspection of the forward angles indicated that some readjustments of about $\pm 10\%$, for ^{96,98,100}Mo might be in order, and were applied. This uncertainty does not appear to affect the conclusions significantly. These data were supplemented with 14.5-MeV proton analyzing-power data,[6] averaged over Zr isotopes. The energies of 11 and 15 MeV have the advantage of differing by the Coulomb correction energy $0.4Z/A^{1/3} \simeq 4$ MeV.

Analysis was made with the search program CUPID.[7] The potentials were similar to those of Ref. 1, consisting of a real volume and imaginary derivative Woods-Saxon central terms and a conventional real spin-orbit term. Each data set showed a preference for the geometry of the real-central and spin-orbit terms to be nearly the same and this constraint was adopted. The spin-orbit well depth was held constant at -24 MeV.[8]

Optical-model searches on the individual data sets revealed some possible systematics regarding the projectile and/or mass dependence of the parameters. These were generally smooth except for occasional irregularities for ^{92,100}Mo. However, the χ^2 fitting parameter was weakly dependent on these trends and it proved to be reasonable and convenient to adopt a common geometry for each data set ($r_0 = r_{s.o.} = 1.20$, $a = a_{s.o.}$